Rev. Roum. Sci. Techn.– Électrotechn. et Énerg.
Vol. **67**, *1*, pp. 65–72, Bucarest, 2022

Automatique et ordinateurs

ADAPTIVE NON-LINEAR VOLTAGE CONTROLLER BASED MULTIVARIABLE SLIDING MODE EXTREMUM SEEKING APPROACH APPLIED TO MULTI-MACHINE POWER SYSTEM

AMEL ABBADI[1*], FETHIA HAMIDIA[1], YOUNES CHIBA[2]

Keywords: Voltage regulation, transient stability enhancement, adaptive controller, Multivariable sliding extremum seeking, Multimachines power system, online gain adjustment.

The goal of this work is to construct an adaptive nonlinear voltage control law using a multivariable sliding extremum seeking (SES) technique. The developed scheme is applied to ensure the transient stability enhancement and the voltage regulation of the multi-machine power system. This control scheme can be depicted as an intelligent adaptive controller. It is a non-model-based method since the multivariable SES approach tunes on-line the gains of the nonlinear voltage controller based on the minimization of a cost function without needing knowledge of the nonlinear model of the multi-machine power system. This cost function represents the performances of the system. The efficiency and effectiveness of the proposed approach are discussed through different multi-machine power systems under different disturbances, initials conditions, and system configurations.

1. INTRODUCTION

Nowadays, the availability and quality of electrical energy have become top concerns for consumers and suppliers. As a result, studying the stability of electrical systems is becoming critically important [1–7]. The excitation control system of the synchronous generators has attracted many research efforts, as it constitutes an effective means for improving the stability of the power system [1–3, 5–7].

Traditional excitation systems are based on automatic voltage regulation and power system stabilizer (AVR/PSS). They are mainly designed by using the theory of linear control, in other terms; the nonlinear model of the system is approximated by a valid linear model in a small region around an operating point [4-7]. But since AVR / PSS are designed separately, regulating voltage, and improving system stability are difficult to be achieved simultaneously. Furthermore, the inconvenience of these types of design approaches is that the designed controllers depend on the operating conditions and may not work properly for modern power systems which are highly complex and nonlinear mainly when a major fault occurs [4].

For the above-mentioned reason, many advanced control techniques have been proposed for designing excitation controllers, such as adaptive control [8-9] where the transient stability is well improved and the voltage regulation response is acceptable, sliding mode control [10,11] and robust control [12] in which both transient stability and voltage regulation are well achieved, Takagi Sugeno fuzzy logic control systems solved through the use of linear matrix inequalities as in [13] or by the synergetic control theory [14]. Also, to ensure transient stability enhancement and voltage regulation, several attempts have been made based on a switching strategy between different control actions [15–17].

All these control systems developed are based on the identification of the installation model to adjust the controller's gains. Our main aim in this article is to propose an improved adaptive nonlinear voltage controller that can achieve both voltage regulation and transient stability enhancement simultaneously and can be easily implementable in real-time by using the sliding extremum seeking control approach which is a model-free real-time optimization strategy. Extremum seeking (ES) algorithm is well suited for systems with unknown dynamics or those affected by high levels of uncertainty and / or external dynamics [18,19].

Recently, the extremum seeking algorithm has been proposed for the adjustment of PID gains [20–22]. The parameters of the PID controller are modified iteratively by minimizing a so-called cost function (J (θ)), which characterizes the desired performance of the system. This approach is considered as an adaptive optimization method in real-time.

In [20–22], the search for the extremum of the cost function is based on the gradient method, which implies that the PID parameters found are not necessarily global minima of J(θ). In addition, due to the high values of gradient magnitude term, the gradient-based ES does not adequately reject the effect of disturbances and parameter variations, which can affect the stability of the multi machine power system.

To overcome the above-mentioned limitations, a new proportional-integral (PI) adjustment method based on sliding mode extremum seeking control scheme is proposed and applied for current control of a brushless PMSM to solve a class of multivariable optimization problem [23]. Indeed, the disadvantage of adjustment of the PI controller parameters with the extremum seeking algorithm based on the gradient method is eliminated by using the sliding mode, which makes the regulator robust against modeling uncertainties and disturbances [24,25].

In this paper, motivated by the advantages of the sliding mode extremum seeking control approach, an adaptive nonlinear voltage controller is proposed to achieve both transient stability enhancement and improvement of voltage regulation of multi-machine power systems. The proposed controller is designed based on several sliding surfaces to optimize the gains of the nonlinear voltage controller through the minimization of an appropriate cost function.

[1] Electrical Engineering Department, Research Laboratory in Electrical Engineering and Automatic LREA, University of Médéa, Médéa, Algeria, *amel.abbadi@yahoo.fr
[2] Faculty of Technology, Department of Mechanical Engineering, University of Médéa, Médéa, Algeria

The remainder of this paper is organized as follows. The dynamic model of the system is briefly described in Section 2. The proposed sliding mode extremum seeking-based adaptive non-linear voltage controller is designed for the multi machines power system in Section 3. The control performance of the proposed controller is verified based on a two-machine infinite-bus power system and a three-machine infinite bus power system respectively in Section 4, followed by Section 5 that concludes this paper.

2. DIRECT FEEDBACK LINEARIZATION COMPENSATED MODEL OF POWER SYSTEM

2.1 DYNAMIC MODEL OF POWER SYSTEM

The third-order single-axis dynamic generator model is widely used in transient stability and voltage regulation studies. In general, for an electrical system with *n*-generator, the dynamic model of the *i*-th generator can be written as follows:

Mechanical equations

$$\dot{\delta}_i(t) = \omega_i(t) - \omega_0, \tag{1}$$

$$\dot{\omega}_i(t) = -\frac{D_i}{2H_i}\left(\omega_i(t) - \omega_0\right) + \frac{\omega_0}{2H_i}\left(P_{mi} - P_{ei}(t)\right). \tag{2}$$

Generator electrical dynamics

$$\dot{E}_{qi}(t) = \frac{1}{T'_{d0i}}\left(E_{fi}(t) - E_{qi}(t)\right). \tag{3}$$

Electrical equations

$$E_{qi}(t) = E'_{qi}(t) + \left(x_{di} - x'_{di}\right)I_{di}(t), \tag{4}$$

$$E_{fi}(t) = k_{ci}u_{fi}(t), \tag{5}$$

$$I_{di}(t) = \sum_{j=1}^{k} E'_{qj}(t)\left(G_{ij}\sin\left(\delta_{ij}(t)\right) - B_{ij}\cos\left(\delta_{ij}(t)\right)\right), \tag{6}$$

$$I_{qi}(t) = \sum_{j=1}^{k} E'_{qj}(t)\left(B_{ij}\sin\left(\delta_{ij}(t)\right) + G_{ij}\cos\left(\delta_{ij}(t)\right)\right), \tag{7}$$

$$P_{ei}(t) = E'_{qi}(t)I_{qi}(t), \tag{8}$$

$$Q_{ei}(t) = E'_{qi}(t)I_{di}(t), \tag{9}$$

$$E_{qi}(t) = x_{adi}(t)I_{fi}(t), \tag{10}$$

$$V_{tdi}(t) = x'_{di}I_{qi}(t), \tag{11}$$

$$V_{tqi}(t) = E'_{qi}(t) - x'_{di}I_{di}(t), \tag{12}$$

$$V_{ti}(t) = \sqrt{V^2_{tqi}(t) + V^2_{tdi}(t)}, \tag{13}$$

where $\delta_i(t)$ the angle of the *i*-th generator, in radian; $\omega_i(t)$ the relative speed of the *i*-th generator, in rad/sec; P_{mi} the mechanical input power, in p.u.; P_{ei} (t) the electrical power, in p.u.; ω_0 the synchronous machine speed**,** in rad/sec, $\omega_0 = 2\pi f_0$; D_i the per unit damper constant; H_i the inertia constant, in seconds. $E'_{qi}(t)$ the transient EMF in quadrature axis, in p.u.; $E_{fi}(t)$ the equivalent EMF in the excitation coil, in p.u.; T'_{doi} the direct axis transient open circuit time constant, in second; E_{qi} the EMF in quadrature axis, in p.u.; V_{ti} the generator terminal voltage, in p.u.; x_{di} the direct axis reactance, in p.u.; x'_{di} the direct axis transient reactance, in p.u.; I_{di} the direct axis current, in p.u.; I_{qi} the quadrature axis current, in p.u.; k_{ci} the gain of the excitation amplifier, in p.u.; u_{fi} the input of the SCR amplifier; x_{adi} the mutual reactance between the excitation coil and the stator coil; $Y_{ij} = G_{ij}+jB_{ij}$ the *i*-th row and *j*-th column element of nodal admittance matrix, in p.u.; Q_{ei} the reactive power, in p.u.; I_{fi} the excitation current.

2.2 FEEDBACK LINEARIZATION COMPENSATION DESIGN

In this paper, the design objective is to improve the voltage regulation and transient stability performance of the multi-machine power system, subjected to severe disturbances. Therefore, the generator terminal voltage must be considered when designing the control law. From the model given above, it can be found that the synchronous generator is nonlinear through the excitation loop. The direct feedback linearization (DFL) technique is designed to cancel the nonlinearities in the electrical equations.

Indeed, by employing the DFL compensating law [12,13]:

$$u_{fi}(t) = \frac{1}{k_{ci}I_{qi}(t)}\left(v_{fi}(t) - T'_{doi}E'_{qi}\dot{I}_{qi} + P_{mi}\right) + \frac{1}{k_{ci}}\left(\left(x_{di} - x'_{di}\right)I_{di}(t)\right), \tag{14}$$

where $v_{fi}(t)$ is the new input.

The DFL compensated system model derived is presented by two subsystems 1 and 2 as follows:

$$1: \begin{cases} \Delta\dot{V}_{ti}(t) = f_{i_1}\Delta\omega_i(t) - \dfrac{f_{i_2}}{T'_{doi}}\Delta P_{ei}(t) + \dfrac{f_{i_2}}{T'_{doi}}v_{fi}(t), \\ y_{1i}(t) = \Delta V_{ti}(t), \end{cases} \tag{15}$$

$$2: \begin{cases} \Delta\dot{\delta}_i(t) = \Delta\omega_i(t), \\ \Delta\dot{\omega}_i(t) = -\dfrac{D_i}{2H_i}\Delta\omega_i(t) - \dfrac{\omega_0}{2H_i}\Delta P_{ei}(t), \\ \Delta\dot{P}_{ei}(t) = -\dfrac{1}{T'_{doi}}\Delta P_{ei}(t) + \dfrac{1}{T'_{doi}}v_{fi}(t), \\ y_{2i}(t) = \Delta\delta_i(t), \end{cases} \tag{16}$$

with

$$f_{i_1} = -\frac{\left(1 + x'_{di}B_{ii}\right)\left[-E'^2_{qi}B_{ii} - Q_{ei}(t)V_{tqi}(t)\right]}{V_{ti}(t)I_{qi}(t)} - \frac{x'_{di}\left(1 + x'_{di}B_{ii}\right)}{V_{ti}(t)}, \tag{17}$$

$$f_{i_2} = -\frac{\left(1 + x'_{di}B_{ii}\right)V_{tqi}(t)}{V_{ti}(t)I_{qi}(t)}, \tag{18}$$

where $f_{i1}(t)$ and $f_{i2}(t)$ are highly nonlinear functions and

$$\Delta\delta_i(t) = \delta_i(t) - \delta_{i0};\ \Delta\omega_i(t) = \omega_i(t) - \omega_0;\ \Delta P_{ei}(t) = P_{ei}(t) - P_{mi}. \tag{19}$$

Full mathematical details and physical assumptions of this model can be found in [12,13,16].

3. ADAPTIVE NON-LINEAR VOLTAGE CONTROLLER BASED MULTIVARIABLE SLIDING MODE EXTREMUM SEEKING APPROACH

3.1 THE COST FUNCTION OF THE SLIDING MODE EXTREMUM SEEKING APPROACH

Now we should define the cost function that will be used by the multivariable sliding extremum seeking approach to deal with the coupling problem of transient stability and voltage regulation. The proposed control scheme is characterized by first defining a suitable pair of sliding surfaces for the first and the second subsystems respectively:

$$S_{1i} = \Delta V_{ti}(t)\ , \tag{20}$$

$$S_{2i} = \left(\frac{d}{dt} + \lambda_i\right)^2 \Delta\delta_i\ \ ,\lambda_i > 0\,. \tag{21}$$

The suggested control strategy must move the states of the

two subsystems towards their sliding surfaces $S_{1i} = 0$ and $S_{2i} = 0$, and eventually, converge to the points $\Delta V_{ti}(t) = 0$ and $\left[\Delta\delta_i(t) \quad \Delta\omega_i(t) \quad \Delta P_{ie}(t)\right]^{\mathrm{T}} = \left[0 \quad 0 \quad 0\right]^{\mathrm{T}}$ respectively. Then, define a hierarchical coupled sliding surface as

$$S_i = S_{1i} - z_i, \tag{22}$$

where z_i is defined as $z_i = \mathrm{sat}\left(S_{2i}/\phi_{zi}\right)Z_u$, $0 < Z_u < 1$ and ϕ_{zi} is the boundary layer of S_{2i} to smooth z, ϕ_{zi} transfers S_{2i} to the proper range of S_{1i}, and the definition of sat(.) function is $\mathrm{sat} = \mathrm{sgn}(\varphi)$, if $|\varphi| \geq 1$, or φ, if $|\varphi| < 1$.

The subsystem 1 involves knowledge of subsystem 2. The adopted cost function, which will quantify the performance of the proposed adaptive nonlinear voltage controller, is

$$y(t) = \frac{1}{T}\int_0^T S_i^2(t)dt. \tag{23}$$

3.1 CONTROLLER DESIGN

Selecting $\boldsymbol{x}_i = \left[\Delta V_{ti}(t) \quad \Delta\omega_i(t) \quad \Delta P_{ei}(t)\right]^{\mathrm{T}}$ as a state vector, the DFL-compensated model adopted (15,16) can be written as follows:

$$\dot{\mathbf{x}}_i(t) = \mathbf{A}_i\boldsymbol{x}_i + \mathbf{B}_i\mathbf{u}_i(t), \tag{24}$$

where

$$\mathbf{A}_i = \begin{bmatrix} 0 & f_{i_1}(t) & -f_{i_2}(t)/T_{d0i} \\ 0 & -D_i/2H_i & -\omega_0/2H_i \\ 0 & 0 & -1/T_{d0i} \end{bmatrix}; \mathbf{B}_i = \begin{bmatrix} -f_{i_2}(t)/T_{d0i} \\ 0 \\ 1/T_{d0i} \end{bmatrix};$$

$$\mathbf{u}_i(t) = \mathbf{v}_{fi}(t).$$

The feedback control law adopted is:

$$v_{fi}(t) = -\boldsymbol{\Gamma}_i^{T}(t)\,\boldsymbol{\theta}_i, \tag{25}$$

where

$$\boldsymbol{\theta}_i = \left[K_{i1}\ K_{i2}\ K_{i3}\right]^{\mathrm{T}};\ \boldsymbol{\Gamma}_i(t) = \left[\Delta V_{ti}(t)\ \Delta\omega_i(t)\ \Delta P_{ei}(t)\right]^{\mathrm{T}} \tag{26}$$

$\boldsymbol{\theta}_i$ and $\boldsymbol{\Gamma}_i(t)$ will be developed to simultaneously solve the control problems of the transient stability enhancement and the voltage regulation.

In our case, the matrices $\mathbf{A}_i$ and $\mathbf{B}_i$ are uncertain ($f_{i_1}(t)$and $f_{i_2}(t)$ are variable). The most appropriate control theory is the free model adaptive control theory such as the extremum seeking method since it alleviates the controller from the knowledge of the system model. The adopted scheme aims to determine the different gains K_{i1}, K_{i2} and K_{i3} by adopting a simplified minimum search method with a periodic switching function.

Assume that there exists an ideal adaptive nonlinear voltage controller $v_{fi}^*(t)$ with optimal gain vector $\theta_i^* = \left[K_{i1}^* K_{i2}^* K_{i3}^*\right]^{\mathrm{T}}$ as follows:

$$v_{fi}^*(t) = -\boldsymbol{\Gamma}_i^{\mathrm{T}}(t)\boldsymbol{\theta}_i^*. \tag{27}$$

The goal is to design an adaptive nonlinear voltage control law such that the tracking errors $\left(\Delta V_{ti}(t),\Delta\omega_i(t),\Delta P_{ei}(t)\right)$ converge to zero as $t \to \infty$. In this case, the adopted controller $v_{fi}(t)$ approximates the ideal unknown $v_{fi}^*(t)$ such that the error

$$e_{v_{fi}}(t) = v_{fi}^*(t) - v_{fi}(t), \tag{28}$$

converges to zero as $t \to \infty$.

The convergence process of $\boldsymbol{\theta}_i$ to $\boldsymbol{\theta}_i^*$ can be divided into three stages as follows [26]:

1. The convergence stage: the system trajectory converges to the sliding mode from an initial value.
2. The forced tracking stage: the system trajectory converges to the extremum point in the sliding mode.
3. The steady-state oscillation stage: the system trajectory remains at a vicinity of the extremum point with oscillation.

The sliding extremum seeking approach adopted is based on the principle of varying the estimated gains $\boldsymbol{\theta}_i$ so that the cost function $J_i(\boldsymbol{\theta}_i)$ reaches the minimum point.

For each generator '*i*' of the multi-machine power system (*k* is the number of the generators in this system), the proposed scheme utilizes three sliding surfaces to optimize the gains K_{i1}, K_{i2}, and K_{i3} of the proposed controller, corresponding respectively to the variation of the generator terminal voltage, rotor speed, and the active electrical power delivered by the generator.

Hence the vector of the switching functions is defined as:

$$\boldsymbol{\sigma}_i(t) = \left[\sigma_{i1}\ \sigma_{i2}\ \sigma_{i3}\right]^T, \tag{29}$$

where

$$\begin{aligned}\boldsymbol{\sigma}_i(t) &= y_i(t) - \mathbf{g}_i(t) \\ &= J_i\left(\theta_{i1}(t),\theta_{i2}(t),\theta_{i3}(t)\right) - \mathbf{g}_i(t),\end{aligned} \tag{30}$$

$\mathbf{g}_i(t)$ is a column vector of increasing functions satisfying:

$$\dot{\mathbf{g}}_i(t) = \mathbf{p}_i(t), \tag{31}$$

and $\mathbf{p}_i(t)$ is a column vector of positive constants.

The parameter θ_{ij} is designed to satisfy:

$$\dot{\theta}_{ij} = K_{ses_{ij}}\,\mathrm{sgn}\left(\sin\left(\pi\sigma_{ij}/\beta_{ij}\right)\right). \tag{32}$$

The derivative of the switching function $\sigma_{ij}(t)$ defined in (29) is

$$\begin{aligned}\frac{\partial}{\partial t}\boldsymbol{\sigma}_{ij}(t) &= \dot{\mathbf{y}}_i(t) - \dot{\mathbf{g}}_i(t) \\ &= \phi_{ij}\left(\boldsymbol{\theta}_i(t)\right)K_{ses_{ij}}\,\mathrm{sgn}\left(\sin\left(\pi\sigma_{ij}/\beta_{ij}\right)\right) - p_{ij},\end{aligned} \tag{33}$$

where y_i(t) is the cost function and $\phi_{ij}\left(\boldsymbol{\theta}_i(t)\right)$ is defined as $\phi_{ij}\left(\boldsymbol{\theta}_i(t)\right) = \partial J_i\left(\boldsymbol{\theta}_i(t)\right)/\partial\theta_{ij}$ where $\phi_{ij}\left(\boldsymbol{\theta}_i(t)\right)$ is the *j*-th element of the vector $\boldsymbol{\varphi}_i\left(\boldsymbol{\theta}_i(t)\right) = \partial J_i\left(\boldsymbol{\theta}_i(t)\right)/\partial\boldsymbol{\theta}_i$.

The sliding control law can be expressed by:

$$\begin{aligned}\dot{\theta}_{ij} &= v_{ij}, \\ v_{ij} &= K_{ses_{ij}}\,\mathrm{sgn}\left(\sin\left(\pi\sigma_{ij}/\beta_{ij}\right)\right).\end{aligned} \tag{34}$$

It is important to point out that for the classic sliding mode, only one sliding mode intervenes; on the other hand, in the extremum seeking control system with sliding mode a series of sliding modes can occur. Therefore, the corresponding switching functions for each θ_{ij} are defined as [27]:

$$\xi_{n_{ij}} = \sigma_{ij}(t) - n\beta_{ij} \quad (i = 1,....k;\ j = 1,2,3). \tag{35}$$

The switching function is satisfying the condition

$$\begin{aligned}&-\beta_{n_{ij}} \leq \xi_{n_{ij}}(t) \leq \beta_{n_{ij}};\ \dot{\xi}_{n_{ij}}(t) = \dot{\sigma}_{ij}(t); \\ &\mathrm{sgn}\left(\xi_{n_{ij}}(t)\right) = -\mathrm{sgn}\left(\phi_{ij}\left(\boldsymbol{\theta}_i(t)\right)\right)\mathrm{sgn}\left(\sin\left(\pi\sigma_{ij}/\beta_{ij}\right)\right).\end{aligned} \tag{36}$$

Remark: In this paper and based on assumption presented in [27,28], the cost function $y_i(t)$ is approximately expressed by $y_i(t) = J_i\left(\boldsymbol{\theta}_i(t)\right)$.

3.2 STABILITY ANALYSIS

To analyze the convergence and stability of the closed-loop system, the following Lyapunov function is considered:

$$V_i = \frac{1}{2}\boldsymbol{\xi}_{n_i}\boldsymbol{\xi}_{n_i}^{\mathrm{T}}, \tag{37}$$

where $\boldsymbol{\xi}_{n_i} = \left[\xi_{n_{i1}}\ \xi_{n_{i2}}\ \xi_{n_{i3}}\right]$.

The derivative of V_i with respect to time is given by:

$$\dot{V}_i = \dot{\boldsymbol{\xi}}_{n_i}\boldsymbol{\xi}_{n_i}^{T} = \sum_{j=1}^{3}\dot{\xi}_{n_{ij}}\xi_{n_{ij}}. \tag{38}$$

The parameter θ_{ij} defined in (32) is designed to satisfy:

$$\dot{\theta}_{ij} = -K_{ses_{ij}}\ \mathrm{sgn}\left(\phi_{ij}\left(\boldsymbol{\theta}_i(t)\right)\right)\mathrm{sgn}\left(\xi_{n_{ij}}\right), \tag{39}$$

from which the derivative of the switching function with respect to time is determined by:

$$\dot{\xi}_{n_{ij}} = -K_{ses_{ij}}\left|\phi_{ij}\left(\boldsymbol{\theta}_i(t)\right)\right|\mathrm{sgn}\left(\xi_{n_{ij}}\right) - p_{ij} \tag{40}$$

This allows that

$$\dot{V}_i = \sum_{j=1}^{3} -\left|\xi_{n_{ij}}(t)\right|\left(\left|\phi_{ij}\left(\boldsymbol{\theta}_i(t)\right)\right|K_{ses_{ij}} + p_{ij}\,\mathrm{sgn}\left(\xi_{n_{ij}}(t)\right)\right). \tag{41}$$

Define a γ_{ij} vicinity $\Omega^*_{i\,j}\left(\gamma_{l\,ij},\gamma_{r\,ij}\right)$ of the maximum point θ^*_{ij} as:

$$\Omega^*_{i\,j}\left(\gamma_{l\,ij},\gamma_{r\,ij}\right) = \left\{\theta_{ij}\left|\theta^*_{ij} - \gamma_{l_{ij}} \le \theta_{ij} \le \theta^*_{ij} + \gamma_{r_{ij}}\right.\right\}, \tag{42}$$

where $\gamma_{l_{ij}}$ and $\gamma_{r_{ij}}$ are positive constante . Then one of the following possibilities holds

$$\begin{aligned}&\left|\phi_{ij}\left(\boldsymbol{\theta}_i(t)\right)\right| > p_{ij}/K_{ses_{ij}}, \quad \forall\theta_{ij} \notin \Omega^*_{i\,j}\left(\gamma_{l\,ij},\gamma_{r\,ij}\right),\\ &\left|\phi_{ij}\left(\boldsymbol{\theta}_i(t)\right)\right| \le p_{ij}/K_{ses_{ij}}, \quad \forall\theta_{ij} \in \Omega^*_{i\,j}\left(\gamma_{l\,ij},\gamma_{r\,ij}\right).\end{aligned} \tag{43}$$

FOR THE FIRST POSSIBILITY

It is assumed that the initial condition $\theta_{ij}(0)$ of the system is outside the γ_{ij} vicinity, *i.e.*,

$$\left|\phi_{ij}\left(\boldsymbol{\theta}_i(0)\right)\right| > p_{ij}/K_{ses_{ij}}. \tag{44}$$

Then, as long as the system is outside the γ_{ij} vicinity, we have

$$\left|\phi_{ij}\left(\boldsymbol{\theta}_i(t)\right)\right| > p_{ij}/K_{ses_{ij}}, \quad \theta_{ij} \notin \Omega^*_{i\,j}\left(\gamma_{l\,ij},\gamma_{r\,ij}\right), \tag{45}$$

and

$$\dot{V}_i = \sum_{j=1}^{3} -K_{ses_{ij}}\left|\xi_{n_{ij}}(t)\right|\left(\begin{array}{l}\left|\phi_{ij}\left(\boldsymbol{\theta}_i(t)\right)\right| +\\ +\dfrac{p_{ij}}{K_{ses_{ij}}}\mathrm{sgn}\left(\xi_{n_{ij}}(t)\right)\end{array}\right) < 0, \tag{46}$$

which indicates that the system will move towards the sliding mode $\xi_{n_{ij}} = 0$.

The equivalent control input can be derived by solving $\dot{\sigma}_{ij}(t) = 0$ for $v_{ij}(t)$:

$$\dot{\sigma}_{ij}(t) = \frac{\partial}{\partial\theta_{ij}}J_i\left(\boldsymbol{\theta}_i(t)\right)v_{eq_{ij}} - p_{ij} = 0. \tag{47}$$

This implies that:

$$v_{eq_{ij}} = \frac{p_{ij}}{\phi_{ij}\left(\boldsymbol{\theta}_i(t)\right)}. \tag{48}$$

Furthermore, note that under the assumption that, the local cost function $J_i\left(\boldsymbol{\theta}_i(t)\right)$ is concave function we have

$$\left(\theta_{ij}(t) - \theta^*_{ij}\right)\frac{\partial J_i}{\partial\theta_{ij}(t)} < 0 \quad , \quad \forall\ \theta_{ij}(t) \neq \theta^*_{ij}. \tag{49}$$

Let $\hat{\theta}_{ij} = \theta_{ij}(t) - \theta^*_{ij}$, the time derivative of $\hat{\theta}_{ij}$ is:

$$\dot{\hat{\theta}}_{ij} = v_{eq_{ij}}. \tag{50}$$

From eqs. (48) and (49), it follows that

$$\hat{\theta}_{ij}(t)\ \dot{\hat{\theta}}_{ij}(t) < 0, \tag{51}$$

that is $\theta_{ij}(t) \to \theta^*_{ij}$ in the region (45) as long as the sliding mode exists, which implies that (28) converges to zero.

FOR THE SECOND POSSIBILITY

In this subsection, we use the switching function $\sigma_{ij}(t)$ to discuss the convergence. Once the sliding mode reached, the system enter the γ_{ij} vicinity, *i.e.*,

$$\left|\phi_{ij}\left(\boldsymbol{\theta}_i(t)\right)\right| \le p_{ij}/K_{ses_{ij}}, \quad \forall\theta_{ij} \in \Omega^*_{i\,j}\left(\gamma_{l\,ij},\gamma_{r\,ij}\right). \tag{52}$$

If $$2n\beta_{ij} < \sigma_{ij}(t) < (2n+1)\beta_{ij} \tag{53}$$

then $$\theta_{ij} = K_{ses_{ij}} > 0. \tag{54}$$

It can be seen that θ_{ij} will continue to increase and two cases may happen.

Case 1: If $p_{ij}/K_{ses_{ij}}$ is designed to be small, before decreases to $\sigma_{ij}(t) = 2n\beta_{ij}$ from $\sigma_{ij}(t) = (2n+1)\beta_{ij}$, the system will cross the region $\left|\phi_{ij}\left(\boldsymbol{\theta}_i(t)\right)\right| \le p_{ij}/K_{ses_{ij}}$ and reach the region $\left|\phi_{ij}\left(\boldsymbol{\theta}_i(t)\right)\right| > p_{ij}/K_{ses_{ij}}$. In this case, the condition of sliding modes comes into existence and the system converges to sliding surface $\sigma_{ij}(t) = 2n\beta_{ij}$ on which the system moves to region $\left|\phi_{ij}\left(\boldsymbol{\theta}_i(t)\right)\right| \le p_{ij}/K_{ses_{ij}}$.

Case 2: If $p_{ij}/K_{ses_{ij}}$ is designed to be large enough, the system is still in the region $\left|\phi_{ij}\left(\boldsymbol{\theta}_i(t)\right)\right| \le p_{ij}/K_{ses_{ij}}$ and σ_{ij} decreases to $\sigma_{ij}(t) = 2n\beta_{ij}$ from $\sigma_{ij}(t) = (2n+1)\beta_{ij}$.

From the sliding surface $\sigma_{ij} = 2n\beta_{ij}$, we can get:

$$(2n-1)\beta_{ij} < \sigma_{ij}(t) < 2n\beta_{ij}, \tag{55}$$

which implies that:

$$\theta_{ij} = -K_{ses_{ij}} < 0. \tag{56}$$

It can be seen that σ_{ij} will continue to decrease and two cases may happen

Case 1: If $p_{ij}/K_{ses_{ij}}$ is designed to be small, the system will cross the region $\left|\phi_{ij}\left(\boldsymbol{\theta}_i(t)\right)\right| \le p_{ij}/K_{ses_{ij}}$ and reach the region $\left|\phi_{ij}\left(\boldsymbol{\theta}_i(t)\right)\right| > p_{ij}/K_{ses_{ij}}$. In this case, the condition of sliding modes comes into existence and the system converges to sliding surface $\sigma_{ij}(t) = (2n-1)\beta_{ij}$ on which the system moves to region $\left|\phi_{ij}\left(\boldsymbol{\theta}_i(t)\right)\right| \le p_{ij}/K_{ses_{ij}}$.

Case 2: If $p_{ij}/K_{ses_{ij}}$ is designed to be large enough, the system is still in the region $\left|\phi_{ij}\left(\boldsymbol{\theta}_i(t)\right)\right| \le p_{ij}/K_{ses_{ij}}$ and σ_{ij} reduces to $\sigma_{ij}(t) = (2n-1)\beta_{ij}$.

When (40) and (41) appear, the direction of movement changes and so do for (42) and (43). The system will repeat those movements near the extreme point.

3. SIMULATION RESULTS

To validate the performances of the developed adaptive nonlinear voltage controller, two different configurations of the multi-machine power systems are considered:

- Three-generator infinite bus power system (Fig.1). The full mathematical details can be found in [10]. The initials conditions are listed in Table 1.
- Two-machine infinite bus power system (Fig.2). The full mathematical details can be found in [12,13]. The initials conditions are listed in Table 2.

The feasibility of the proposed controller is verified by the Matlab software environment.

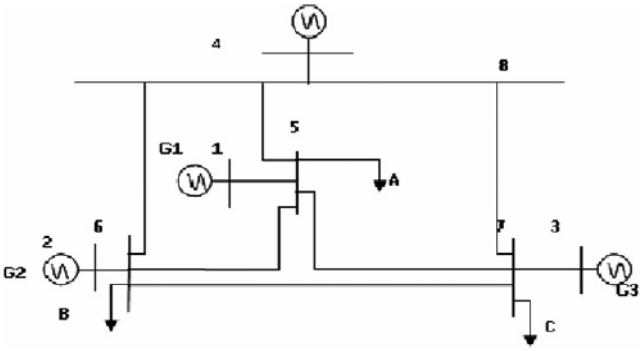

Fig. 1– A three-machine infinite bus power system.

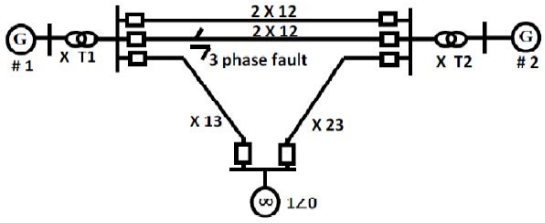

Fig. 2 – A two-machine infinite bus power system.

Table 1

Initial conditions.

Machine	δ(◦)	$P_m(p.u)$	$E_f(p.u)$	$V_t(p.u)$
1	37.93	0.8005	0.3770	0.9999
2	32.07	0.6863	0.4513	1.0200
3	20.88	0.5004	0.6077	1.0399

Table 2

Initial conditions.

Machine	δ(◦)	$P_m(p.u)$	$V_t(p.u)$
1	52.72	0.95	1.00
2	54.48	0.95	1.02

3.1. THREE-GENERATOR INFINITE BUS POWER SYSTEM

In this configuration, the fault considered is a permanent fault with sudden increase in mechanical input power (Fig. 3, 4 and 5). First, a symmetrical three-phase short circuit on the transmission lines between buses 5 and 6 is applied at t = 1s (Fault location λ = 0.2). This fault is eliminated by the opening the breakers of the faulted line at 1.15 s. Secondly the mechanical input power of generator # 1 has increase of 30 %. This rise is applied at t = 1.5 s.

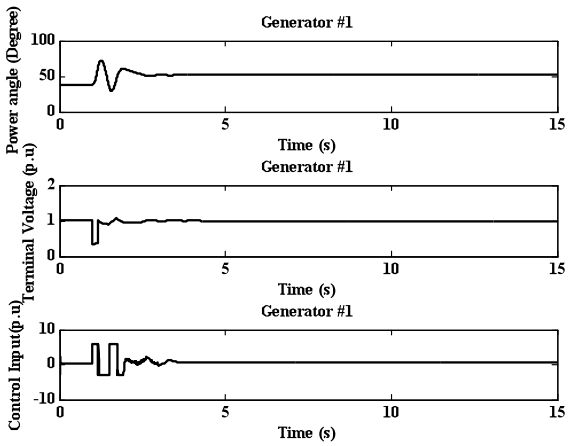

Fig. 3 – System state responses of the generator 1 of the three-generator connected to the infinite bus power system.

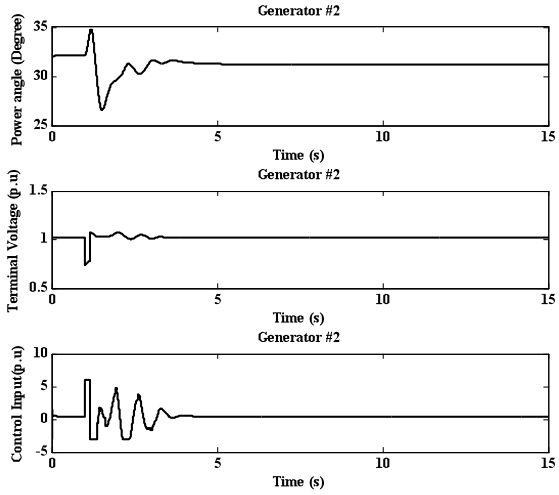

Fig. 4 – System state responses of the generator 2 of the three-generator connected to the infinite bus power system.

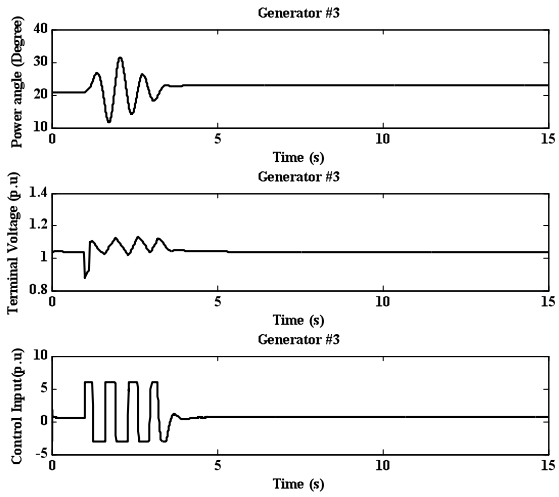

Fig. 5 – System state responses of the generator 3 of the three-generator connected to the infinite bus power system.

Figures 6-8 show the variations of controllers' gains of the system three generators connected to the infinite bus power system.

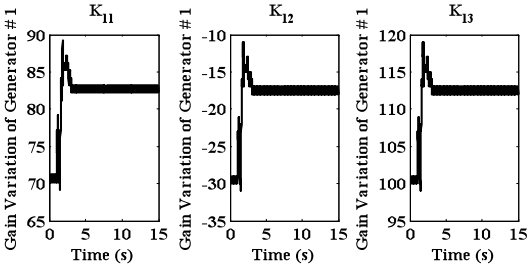

Fig. 6 – Controller's gains variations of the generator 1.

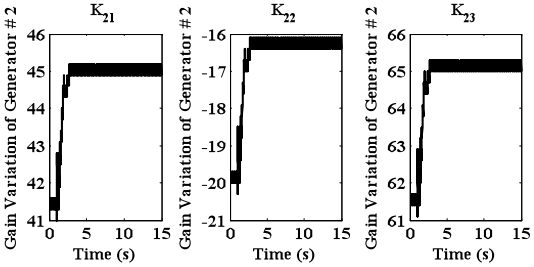

Fig. 7 – Controller's gains variations of the generator 2.

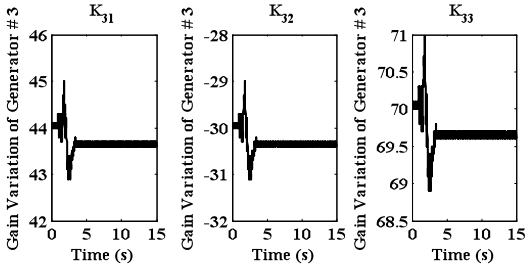

Fig. 8 – Controller's gains variations of the generator 3.

3.2 TWO-MACHINE INFINITE BUS POWER SYSTEM

The simulation is performed for two successively, symmetrical three-phase short circuit fault (location $\lambda = 0.01$). The first fault happens at $t = 1$s. This fault is eliminated by the opening the breakers of the faulted line at $t = 1.15$ s. The transmission lines are restored at $t = 2.5$ s. The second fault occurs at $t = 3.15$ s. The fault is removed by opening the breakers of the faulted line at $t = 3.15$ s (Fig. 9 and Fig. 10).

In order to evaluate the performance of the proposed adaptive nonlinear voltage controller (Adapt Non Vol C) more accurately, the state responses of the proposed controller are compared to those of the robust nonlinear voltage Controller (Rob Non Vol C) described in [12].

Zhu et *al* in [12], have developed a robust nonlinear voltage controller based on the direct feedback linearization (DFL) technique and the robust control theory. The proposed controller is expressed as:

$$\begin{aligned} v_{f1} &= 22.4\Delta\delta_1(t) + 12.8\Delta\omega_1(t) - 82.5\Delta P_{e1}(t), \\ v_{f2} &= 22.4\Delta\delta_2(t) + 14.2\Delta\omega_2(t) - 82.6\Delta P_{e2}(t). \end{aligned} \quad (57)$$

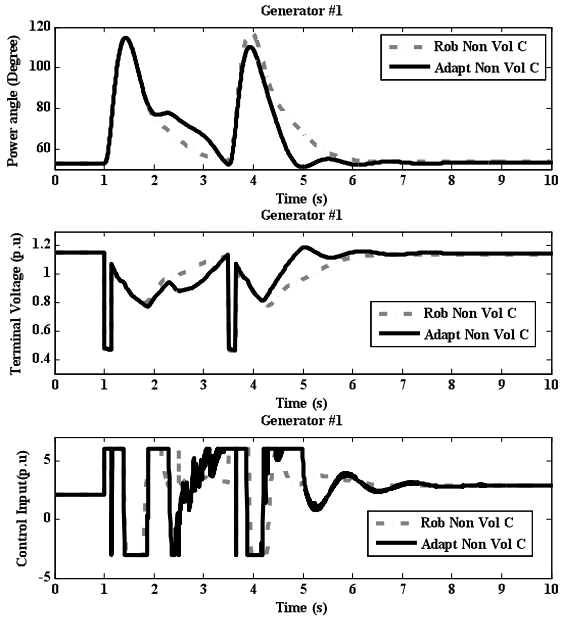

Fig. 9 – System state responses of the generator 1 of the two-generator infinite bus power system.

It can be seen from Figs. 3-5 and Figs. 9-10 that the control tasks tackled are satisfactorily achieved. Indeed, the transient stability is improved, and the generator terminal voltages were well regulated in all cases, which confirm the effectiveness of the proposed approach.

The deviation of the generator terminal voltage (ΔV) and the deviation of power angle ($\Delta\delta$) levels are used to evaluate the performances of the proposed controller and the robust nonlinear voltage controller proposed in [12]. For this comparison, three indices are used, namely the Integral square error (*ISE*), the integral of absolute error (*IAE*) and the integral of time multiplied by absolute error (*ITAE*). The simulation time T is set at 20 s and the results of this comparison are reported in Tables 3 and 4.

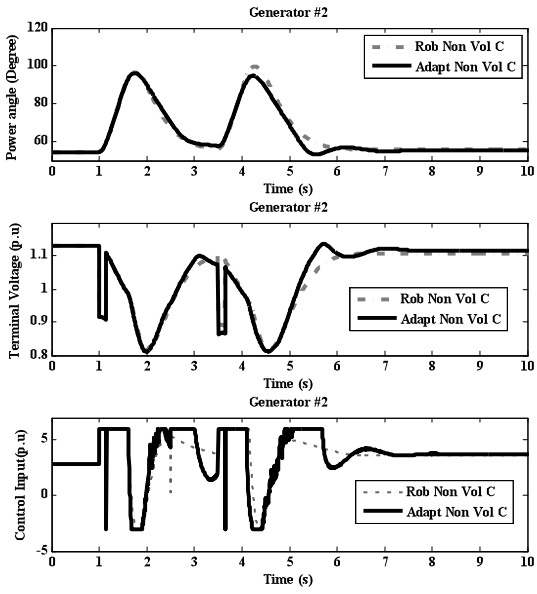

Fig. 10 – System state responses of the generator 2 of the two-generator infinite bus power system.

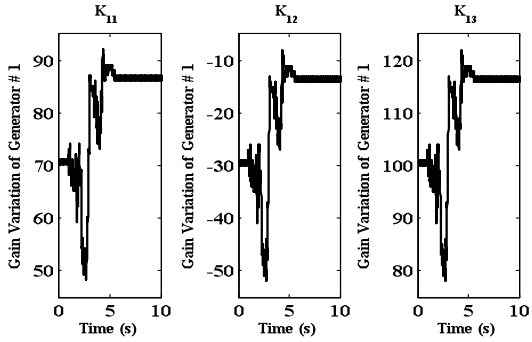

Fig. 11 – Controller's gains variations of the generator 1 for the case 1.

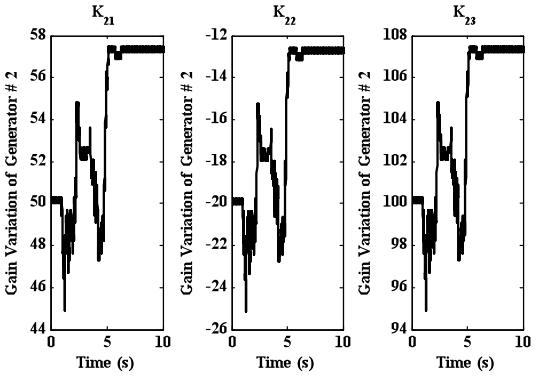

Fig. 12 – Controller's gains variations of the generator 2.

Figures 11 and 12 show the variations of controllers' gains of the system two generators connected to an infinite bus power system.

Table 3

Values of performance indices under different conditions for transient stability evaluation

System responses	Comparator indices of transient stability (Δδ)		
	ITAE	IAE	ISE
Rob Non Vol C	3.8109e+03	835.2794	447.6468
Adapt Non Vol C	2.7822e+03	732.0862	397.9413

Table 4

Values of performance indices under different conditions for voltage regulation evaluation

System responses	Comparator indices of voltage regulation (ΔV)		
	ITAE	IAE	ISE
Rob Non Vol C	2.5006e+03	470.1989	103.5874
Adapt Non Vol C	1.7506e+03	405.1086	100.5577

As shown in Tables 3 and 4, all performance indices confirm that the proposed controller gives better performances compared to the robust nonlinear voltage controller in term of fast convergence responses with better damping of power system oscillations, and minimum steady state error (the system responses of proposed controller are closer to the set points).

Furthermore, according to Figs. 3-5 and Figs. 9,10 the chattering observed on the controller's gains (Figs. 6-8 and Figs. 11,12) has no effect on the control law applied. Therefore, chattering is no longer a big issue in the proposed control scheme since multiple sliding surfaces are applied.

4. **CONCLUSION**

In this article, an adaptive control law based on multivariable sliding extremum seeking approach is used to ensure control and stability of multi-machine power systems. One of the main advantages of this technique is to introduce an approach that requires little or no knowledge of the system model. Moreover, it is not even important if the model of the system is linear or nonlinear as in our case. We only need the cost function that characterizes the desired behavior. Despite the non-linearity and the time-varying properties of the multi-machine power system, the proposed adaptive nonlinear voltage controller via the multivariable SES approach satisfactorily addressed it. Indeed, the transient stability is greatly improved by the proposed controller and the post-fault voltage level is reached despite the different operating points, faults locations, and changes in the mechanical input power, and this for the different multi-machine power systems. Simulation results reveal the superiority of the proposed technique over the robust approach since the proposed controller has a faster convergence speed with less oscillation, and where the steady state responses of system are closer to the set points.

In a general way, it is important to emphasize that the joint use of the sliding extremum seeking technique with any regulator offers a very appreciable flexibility and ease of design in the field of controlling linear systems just as much as non-linear systems since we just need to find the cost function that can represent the desired dynamics of the system and use the technical ES to minimize it.

Received on September 10, 2020

REFERENCES

1. P. Kundur, *Power system stability and control*. McGraw-Hill, New York, 1994.
2. A. Abdelaziz, K. Keltuom, *Power system stabilizer based on terminal sliding mode control*, Rev. Roum. Sci. Techn.– Électrotechn. et Énerg, **62**, *1*, pp. 98–102 (2017).
3. K.R. Padiyar, *Power System Stability and Dynamics*, second edition, BS Publications, 2002.
4. P. Kundur, J. Paserba, V. Ajjarapu, G. Andersson, A. Bose, C. Canizares, N. Hatziargyriou, D. Hill, *Definition, and classification of power system stability*. IEEE Trans. Power Syst., **19**, *2*, pp. 1387–1401(2004).
5. H. Labdelaoui, F. Boudjema, D. Bouthetala, *Multiobjective optimal design of dual-input power system stabilizer using genetic algorithms*. Rev. Roum. Sci. Techn.– Électrotechn. et Énerg, **62**, *1*, pp. 93–97 (2017).
6. A.D. Falehi, M. Rostami, H. Mehrjardi, *Transient Stability Analysis of Power System by Coordinated PSS-AVR design based on pso technique*, Engineering, **3**, *4*, pp. 478-484 (2011).
7. A. Zebar, A. Hamouda, K. Zehar, Impact of the lo*cation of fuzzy controlled static VAR compensator on the power system transient stability improvement in presence of distributed wind generation*, Rev. Roum. Sci. Techn. – Électrotechn. et Énerg., **60**, *4*, pp. 426–436, (2015).
8. R. Yan, Z.Y. Dong, T.K. Saha, R. Majumder, *Power system transient stability enhancement with an adaptive control scheme using backstepping design*, IEEE Power Engineering Society General Meeting, June, pp. 1-8 (2007).
9. S. Abazari, M. Heidari, N.R. Abjadi, *Adaptive control design for a synchronous generator,* Rev. Roum. Sci. Techn. – Électrotechn. et Énerg. **59**, *4*, pp. 411-421(2014).
10. S. Benahdouga, D. Boukhetala, F. Boudjema, *Decentralized high order sliding mode control of multimachine power systems*, Int. J. Electr Power Energy Syst., **43**,*1*, pp.1081-1086 (2012).
11. H. Huerta, A.G. Loukianov, J.M. Cañedo, *Decentralized sliding mode block control of multimachine power systems*, Int. J. Electr. Power Energy Syst. **32**, *1*, pp.1-11 (2010).
12. C. Zhu, R. Zhou, Y. Wang, *A new decentralized nonlinear voltage controller for multimachine power systems*, IEEE Trans. Power Syst. **13**, *1*, pp. 211-216 (1998).
13. A. Abbadi, L. Nezli, D. Boukhetala, *A nonlinear voltage controller based on interval type 2 fuzzy logic control system for multimachine power systems*, Int. J. Electr. Power Energy Syst., **45**, pp. 456-67 (2013).
14. P. Zhao, W. Yao, J. Wen, L. Jiang, S. Wang, S. Cheng, *Improved*

synergetic excitation control for transient stability enhancement and voltage regulation of power systems, Int. J Electr. Power Energy Syst., **68**, pp. 44–51 (2015).
15. Y. Wang, D.J. Hil, *Robust nonlinear coordinated control of power systems*, Automatica, **32**, pp. 611-618 (1996).
16. Y. Guo, D.J. Hill, Y. Wang, *Global transient stability and voltage regulation for power systems*, IEEE Trans. on Power Systems, **16**, *4*, pp. 678-688 (2001).
17. R. Chaudhary, A.K. Singh, *Transient stability improvement of power system using non-linear controllers*, Energy and Power Engineering, **6**, *1*, pp.10–16 (2014).
18. M. Kristic, *Extremum seeking control*, in T. Samad and J. Baillieul, Encyclopedia of Systems and Control, Springer, 2014.
19. K.B. Ariyur, M. Krstic, *Real-time optimization by extremum-seeking control*, Wiley-Interscience, 2003.
20. T. Roux-Oliveira, L.R. Costa, A.V. Pino, P. Paz, *Extremum seeking-based adaptive PID control applied to neuromuscular electrical stimulation*, Medicine, Biology, Analis da Academia Brasileira de Ciencias, **91**, pp. 1-20 (2019).
21. N.J. Killingsworth, M. Krstic, *PID tuning using extremum seekin*'. IEEE Control Systems Magazine, IEEE Control Syst, **26**, *1*, pp. 70-79 (2006).
22. Q. Chen, Y. Tan, J. Li, I. Mareels, *Decentralized PID control design for magnetic levitation systems using extremum seeking*, IEEE Access, **6**, pp. 3059–3067 (2018).
23. S.F Toloue, S.H Kamali, M. Moallem, *Multivariable sliding-mode extremum seeking PI tuning for current control of a PMSM*. IET Electric Power Applications. 14, 3, pp. 348-356 (2020).
24. B. Ouamri, A.F. Zoubir, *Comparative analysis of robust controller based on classical proportional-integral controller approach for power control of wind energy system*, Rev. Roum. Sci. Techn. – Électrotechn. et Énerg., **63**, *2*, pp. 210-216, (2018)
25. G. Bartolini, L. Fridman, A. Pisano, E. Usai. *Modern Sliding Mode Control Theory*. *New Perspectives and Applications*, *lectures note in control and information sciences*, Springer, Berlin Heidelberg, Germany, 2008.
26. S. Chen, L. Wang, K. Ma, H. Zhao, A switching-based extremum seeking control scheme, Int. J. Control, 90, 8, pp. 1688-1702 (2017).
27. Y. Pan, Ü. Özgüner, T. Acarman, Stability and performance improvement of extremum seeking control with sliding mode, Int. J. Control, 76, 9-10, pp. 968–985 (2003).
28. S. Chen, L. Wang, K. Ma, H. Zhao, *A switching-based extremum seeking control scheme*, Int. J. Control, **90**, *8*, pp. 1688-1702 (2016).